Mon. Not. R. Astron. Soc. **000**, 000–000 (0000) Printed June 30, 2016 (MN LATEX style file v2.2)

The origin of most massive black holes at high-z: BLUETIDES and the next quasar frontier

Tiziana Di Matteo[1], Rupert A.C. Croft[1], Yu Feng[2], Dacen Waters[1], Stephen Wilkins[3]
[1] *McWilliams Center for Cosmology, Physics Dept., Carnegie Mellon University, Pittsburgh PA, 15213, USA*
[2] *Berkeley Center for Cosmological Physics, University of California at Berkeley, Berkeley, CA 94720, USA*
[3] *Astronomy Centre, Department of Physics and Astronomy, University of Sussex, Brighton, BN1 9QH, UK*

arXiv:1606.08871v1 [astro-ph.GA] 28 Jun 2016

June 30, 2016

ABSTRACT

The growth of the most massive black holes in the early universe, consistent with the detection of highly luminous quasars at $z > 6$ implies sustained, critical accretion of material to grow and power them. Given a black hole seed scenario, it is still uncertain which conditions in the early Universe allow the fastest black hole growth. Large scale hydrodynamical cosmological simulations of structure formation allow us to explore the conditions conducive to the growth of the earliest supermassive black holes. We use the cosmological hydrodynamic simulation BLUETIDES, which incorporates a variety of baryon physics in a $(400h^{-1}\mathrm{Mpc})^3$ volume with 0.7 trillion particles to follow the earliest phases of black hole critical growth. At $z = 8$ the most massive black holes (a handful) approach masses of $10^8\,\mathrm{M}_\odot$ with the most massive (with $M_{\rm BH} = 4\times10^8\,\mathrm{M}_\odot$) being found in an extremely compact spheroid-dominated host galaxy. Examining the large-scale environment of hosts, we find that the initial tidal field is more important than overdensity in setting the conditions for early BH growth. In regions of low tidal fields gas accretes 'cold' onto the black hole and falls along thin, radial filaments straight into the center forming the most compact galaxies and most massive black holes at earliest times. Regions of high tidal fields instead induce larger coherent angular momenta and influence the formation of the first population of massive compact disks. The extreme early growth depends on the early interplay of high gas densities and the tidal field that shapes the mode of accretion. Mergers play a minor role in the formation of the first generation, rare massive BHs.

1 INTRODUCTION

It is now well established that the properties of supermassive black holes (SMBH) found at the centers of galaxies today are tightly coupled to those of their hosts implying a strong link between black hole and galaxy formation. The strongest direct constraint on the high-redshift evolution of SMBHs comes from the observations of luminous quasars at $z \sim 6$ in the Sloan Digital Sky Survey (SDSS) (Fan et al. 2006; Jiang et al. 2009) and more recently the highest redshift quasar discovered at $z \sim 7$ (Mortlock et al. 2011). No quasars have yet been observed at higher redshifts. Although extremely rare (the comoving space density of $z \sim 6$ quasars is roughly $n \sim$ a few Gpc^{-3}) the inferred hole masses of these quasars are in excess of 10^9 $\mathrm{M}_\odot$, comparable to the masses of the most massive black holes in the Universe today. The origin of the seeds for these black holes and the physical conditions that allow early growth to supermassive black holes therefore remain a challenging problem.

In order to have had sufficient time to build up via gas accretion and BH mergers (resulting from the hierarchical merging of their host halos) the first 'seed' black holes must have appeared at early epochs, $z > 10$. The origin and nature of this seed population remain uncertain. Two distinct populations of seed masses, in the range of $100 - 10^5$ $\mathrm{M}_\odot$ have been proposed: the small mass seeds are usually thought to be the remnants of the first generation of PopIII stars formed from metal-free gas at $z \sim 20 - 30$ (e.g. Bromm, Coppi & Larson 1999; Abel, Bryan & Norman 2000; Nakamura & Umemura 2001; Yoshida et al. 2003; Gao et al. 2006), while the large seeds form by direct dynamical collapse in metal-free galaxies (Koushiappas, Bullock & Dekel 2004; Begelman, Volonteri & Rees 2006, although see also Mayer et al. 2010 for direct collapse into a massive blackhole in the metal-enriched regime).

Growing the seeds to $10^9\,\mathrm{M}_\odot$ in less than a billion years requires extremely large accretion rates - as mergers between black holes are too rare and too inefficient for significant growth. For a black hole accreting at the critical Eddington accretion rate its luminosity $L_{\rm Edd} = (4\pi G c m_p)/\sigma_T M_{BH} = \eta \dot{M}_{\rm Edd} c^2$ (where G, c, m_p and σ_T are the gravitational constant, speed of light, proton mass and Thomson cross section, and η is the standard accretion efficiency) implies exponential growth at the characteristic Eddington timescales, $t_{\rm Edd} = 450\eta/(1-\eta)$ Myr, such that $M_{\rm BH} = M_{\rm seed} e^{t/t_{\rm Edd}}$. For a seed mass ranging from $M_{\rm seed} \sim 100 - 10^5\,\mathrm{M}_\odot$ this

© 0000 RAS

requires $10-17$ e-foldings to reach $M_{\rm BH}\sim 10^9\,{\rm M}_\odot$. The crucial question (for any given seed model) is then where (if at all, or in which kind of halos) and how such vigorous accretion can be sustained at these early times.

As bright quasars are likely to occur in extremely rare high-density peaks in the early universe, large computational volumes are needed to study them. In Di Matteo et al. (2012) we used the MassiveBlack simulation, a cosmological hydrodynamic simulation covering a volume $(0.75\,{\rm Gpc})^3$ appropriate for studying the rare first quasars to show that steady high density cold gas flows responsible for assembling the first galaxies produce the high gas densities that lead to sustained critical accretion rates and hence rapid growth commensurate with the existence of $\sim 10^9\,{\rm M}_\odot$ black holes as early as $z\sim 7$. Here we use our newest, higher resolution cosmological hydrodynamic simulation, BlueTides(Feng et al. 2016, 2015; Waters et al. 2016a,b) (covering a volume of $[0.5\,{\rm Gpc}]^3$) which includes improved prescriptions for star formation, as well as black hole accretion and associated feedback processes. We focus on earlier times, searching for the conditions that allow rapid growth of the massive black holes beyond currently observed redshifts ($z>7$). This also allows us to make predictions for the most massive black holes to be discovered in the near future. Large volume simulations such as *MassiveBlack* (Di Matteo et al. 2012) and associated high-resolutions zooms (Feng et al. 2014) already showed that the existence of the $z=6$ SDSS quasar population, is consistent with our standard structure formation models. Crucially, the BlueTidessimulation with its increased resolution, allows us to study reliably the formation of massive black holes at even earlier times. It therefore provides a unique framework to study the formation of the next frontier of first quasars.

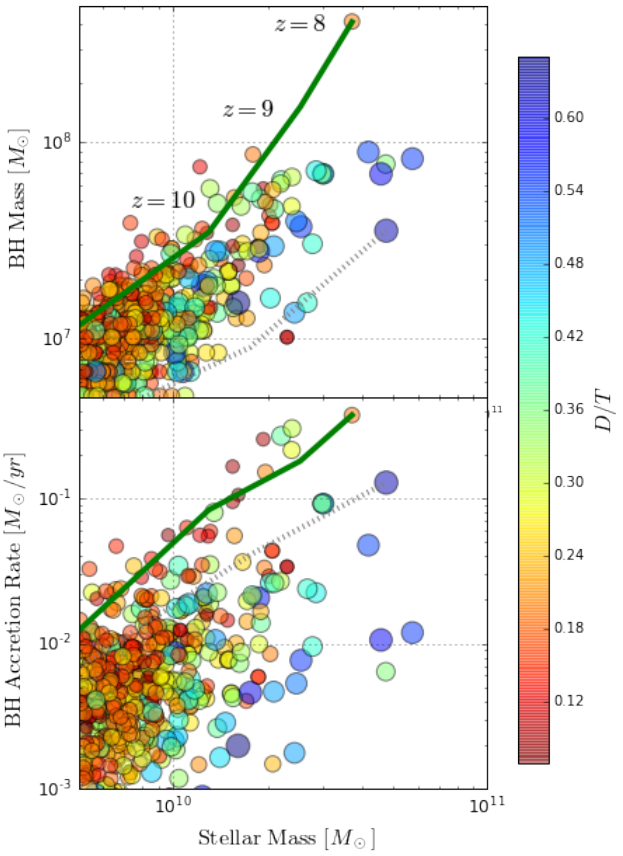

Figure 1. Top panel: Black hole mass versus host galaxy stellar mass at $z=8$. Colors indicate the disk to total (bulge plus disk) ratio for the stellar component, so that blue colors indicate disks and yellow/orange spheroid dominated hosts. The most massive black hole at $z=8$ in BlueTides has a mass of $M_{\rm BH}=4\times10^8\,{\rm M}_\odot$ and resides in a spheroidal host. There are about half a dozen black holes with masses close to $10^8\,{\rm M}_\odot$. The green and dashed track show the redshift evolution of the most massive BH and a massive disk in this plane.

2 BLUETIDES SIMULATION

The BlueTides simulation (see Feng et al. 2015, 2016) for a full description) was carried out using the Smoothed Particle Hydrodynamics code MP-Gadget with 2×7040^3 particles on the Blue Waters system at the National Centre for Supercomputing Applications. The simulation evolved a $(400/h)^3\,{\rm cMpc}^3$ cube to $z=8$ by which time it contained approximately 200 million objects (of which 160,000 have stellar masses greater than $10^8\,{\rm M}_\odot$). At $z=12$ the number of objects identified falls to around 20 million, and only around 30000 have stellar masses greater than $10^{10}\,{\rm M}_\odot$. The galaxy stellar mass and rest-frame UV luminosity functions predicted by the simulation (Feng et al. 2015, 2016; Waters et al. 2016a; Wilkins et al. 2016b,a) match observational constraints available at $z=8,9,10$ (e.g Bouwens et al. 2015; Song et al. 2015). The large volume of BlueTides, almost 200 times larger than either the Illustris, (Vogelsberger et al. 2014) or EAGLE, (Schaye et al. 2015) simulations, makes it ideally suited to an investigation of rare objects at high-redshift. The high resolution (comparable to Illustris) also allows the study of the formation of the first (massive galaxies) and details of the structure and gas inflows inside galaxies. BlueTides was run assuming the Wilkinson Microwave Anisotropy Probe nine year data release (Hinshaw et al. 2013). The simulation is described in more detail in (Feng et al. 2015, 2016) while the physical and observed properties of the galaxy population and predictions for the black hole AGN populations and luminosity functions are described in detail in (Feng et al. 2015, 2016; Wilkins et al. 2016c,b; Waters et al. 2016a,b). In producing galaxy photometry we assume a Chabrier (2003) initial mass function and utilise the Pegase.2 stellar population synthesis model (Fioc & Rocca-Volmerange 1997).

A variety of sub-grid physical processes were implemented to study their effects on galaxy formation:

- star formation based on a multi-phase star formation model (Springel & Hernquist 2003) with modifications following Vogelsberger et al. (2013)
- gas cooling through radiative processes (Katz, Weinberg & Hernquist 1996) and metal cooling (Vogelsberger et al. 2014)
- formation of molecular hydrogen and its effects on star formation (Krumholz & Gnedin 2011)
- type II supernovae wind feedback (the model used in Illustris(Nelson et al. 2015))
- Black growth and AGN feedback using the same model

as in MassiveBlack I and II (Di Matteo, Springel & Hernquist 2005)

- a model of "patchy" reionization (Battaglia et al. 2013) yielding a mean reionization redshift $z \approx 10$ (Hinshaw et al. 2013), and incorporating the UV background estimated by Faucher-Giguère et al. (2009)

In Feng et al. (2015) we performed a standard kinematic decomposition of the stellar component in the galaxies to determine the fraction of stars in each galaxy which are on planar circular orbits, and which are associated with a bulge. We note that this technique is not sensitive to the clumpiness of disks. This provides kinematically classified disks and bulges and a Disk to Total (D/T) ratio for our galaxy sample above a mass of $10^{10}\,\mathrm{M}_{\odot}$ (which contains a sufficient number of stellar particles for this decomposition to be carried out).

Here we also add a calculation of the large scale tidal field. The tidal field can be characterized by three eigenvalues of the local tidal tensor, $t1$, $t2$ and $t3$ (by definition $t1 > t2 > t3$) and the corresponding eigenvectors **t1**, **t2** and **t3**. The three eigenvalues satisfy $t1+t2+t3 \equiv 0$ so that $t1$ is always positive and $t3$ negative. Thus the tidal field stretches material along $t1$ and compresses material along $t3$. By using $t1$ as the indicator of the local tidal field strength we are following standard usage. We define the tidal field as the trace-less part of the strain tensor

$$T_{ij} = S_{ij} - \frac{1}{3}\sum_i S_{ii}, \tag{1}$$

where the strain tensor S_{ij} is the second derivative of the potential ϕ,

$$S_{ij} = \nabla_i \nabla_j \phi. \tag{2}$$

The large scale strain tensor is calculated in Fourier space, following the procedures in Dalal et al. (2008),

$$\hat{S}_{ij} = \frac{k^2}{k_i k_j}\hat{\delta}. \tag{3}$$

We assign the a uniform 1/1000th subsample of the BlueTides particles to the a mesh of 512 grid points per side by a Cloud-in-Cell window (Hockney & Eastwood 1981). The density field is smoothed by a Gaussian window $\exp -0.5k^2s^2$ with a width of $s = 1, 2, 5\,h^{-1}$Mpc. The strain tensor value on the mesh is re-sampled at the location of the central black hole particles by a Cloud-in-Cell window. We note that our definition is different from Wang et al. (2011), where the calculation is performed in configuration space from the nearest neighbour galaxies.

3 RESULTS

3.1 The early assembly of most massive black holes

We turn directly to the most massive black hole population in the galaxies in Bluetides. The left panel of Figure 1 shows black hole mass versus stellar mass of the the host galaxies at $z = 8$. The colours of the points indicate the D/T ratio for the stellar component of each galaxy. The most massive black hole in BlueTides has a mass of $4 \times 10^8\,\mathrm{M}_{\odot}$ at $z = 8$. Interestingly, the most extreme BH does not appear to be hosted by the largest galaxy, in terms of stellar mass, and it has a signifcantly more dominant spheroidal component (D/T only 0.3) than most of the more massive galaxies Feng et al. (2015). The most massive black hole is (positively) offset from the main $M_{BH} - M_*$ relation defined by the rest of the population indicating a relatively faster growth of the black hole compared to the stellar host, as expected. There are a handful of objects with $M_{\rm BH}$ approaching $10^8\,\mathrm{M}_{\odot}$, and only a couple of those in the most massive galaxies with $D/T > 0.5$. A large fraction of the massive black hole population is hosted in intermediate stellar mass hosts with relatively dominant spheroidal components. Examining the left panel of Figure 1 we can see by that both the orange points (spheroids) and blue points (disks) follow a relationship between stellar mass and black hole mass, but that the locus of the spheroidal dominated galaxies is above (higher BH mass) the disks.

Looking at the black hole accretion rates (right panel of Figure 1) we can see that the largest black hole accretion rates are also typically found in the black holes hosted in the more spheroidal galaxies. The locus of black hole accretion rate versus stellar mass for the spheroids is also displaced towards higher black hole mass. In summary therefore, for a given stellar mass, the majority of the most massive black holes seen at $z = 8$, and those accreting at the largest rates, appear to be hosted by (extremely compact) spheroidal dominated galaxies. In Feng et al. (2015) we discussed the population of massive galaxies with significant disk components.

3.2 Examples of high-z massive black holes

3.2.1 Environments

To illustrate the environments and corresponding host galaxy morphologies of the most massive black holes, we show in Figure 2 images of 3 regions containing the most massive black holes in the simulation at $z = 8$. In Figure 3 we compare the environment and host of the most massive black hole in BlueTides(with $\dot{M}_{\mathrm{m}_{BH}} 4 \times 10^8\,\mathrm{M}_{\odot}$) with that of one of the massive disks, as discussed in Feng et al. (2015). For both figures, the images show the projected gas density after zooming into scales 6 h^{-1}mpc, 3 h^{-1}mpc and 0.5 h^{-1}mpc on a side (for left, center and right image in each set respectively). The final inset in the right panel shows the central galaxy host (adaptively smoothing the star particle distribution and color coding according to SFR). The positions of the black holes in all images are indicated with white crosses the sizes of which are proportional to black hole mass. It is interesting to note that only one of these massive black holes is close to undergoing a major merger, and all other massive black holes appear to be associated with isolated high density regions. It is also evident from these images that the most massive black holes strongly favour quasi-spherically collapsed regions of the density field and in turn that such environments are more conducive to the formation to spheroid dominated systems rather than disk dominated stellar hosts. The massive disk-dominated galaxies also host black holes but generally the black hole mass is not amongst the most massive at these epochs. We quantify the origin of the massive galaxy morphology and related black hole growth in Section 3.3.

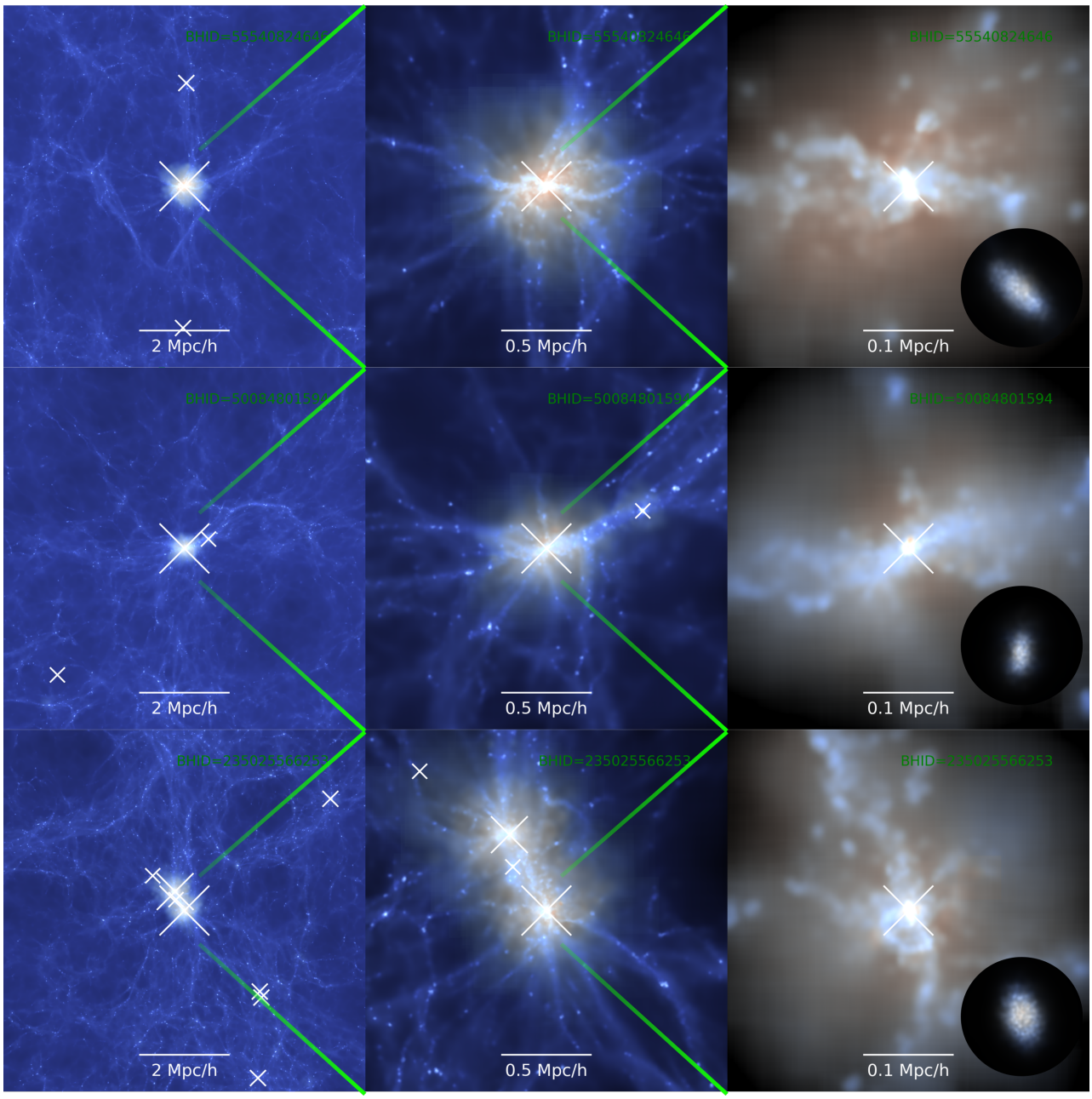

Figure 2. The environments of the most massive $z = 8$ black holes in BlueTides. The images show the large scale gas density around the black holes, zooming into regions of width 6 h^{-1}mpc (left panels) to 3 h^{-1}mpc (center) and 0.5 h^{-1}mpc (right). The gas density field is color coded by temperature (blue to red indicating cold to hot respectively). The final zoom on the top right column show the stellar density for the host galaxy. The positions of the black holes in all images are indicated with white crosses the sizes of which are proportional to black hole mass.

3.2.2 Evolution

In this section we study the evolution of a number of properties for the most massive black holes and compare them to those of some of the most massive stellar systems. Figure 4 shows the co-evolution from $z = 12$ to $z = 8$ of black hole mass and stellar mass for the sample of the four most massive black holes at $z = 8$ shown in Figure 2 and Figure 3 (solid lines). Each line represent a single black hole as it moves from the lower left region and ends up in the top right. The x-axis is the corresponding stellar mass of its host galaxy. For comparison, the dashed lines show the tracks for three other black holes which reside in some disk-dominated hosts (one of which is shown in the top panel of Fig. 3). The tracks of black hole mass versus stellar mass are steeper for the most massive black holes indicating a relatively faster black hole growth than host stellar mass growth comparedfor example to the disk-dominated systems. The latter reside in the most massive stellar systems (dashed lines) which instead tend to grow in stellar mass relatively faster than in black hole mass. At this early time, a very rapid phase of black hole growth is required in order to ex-

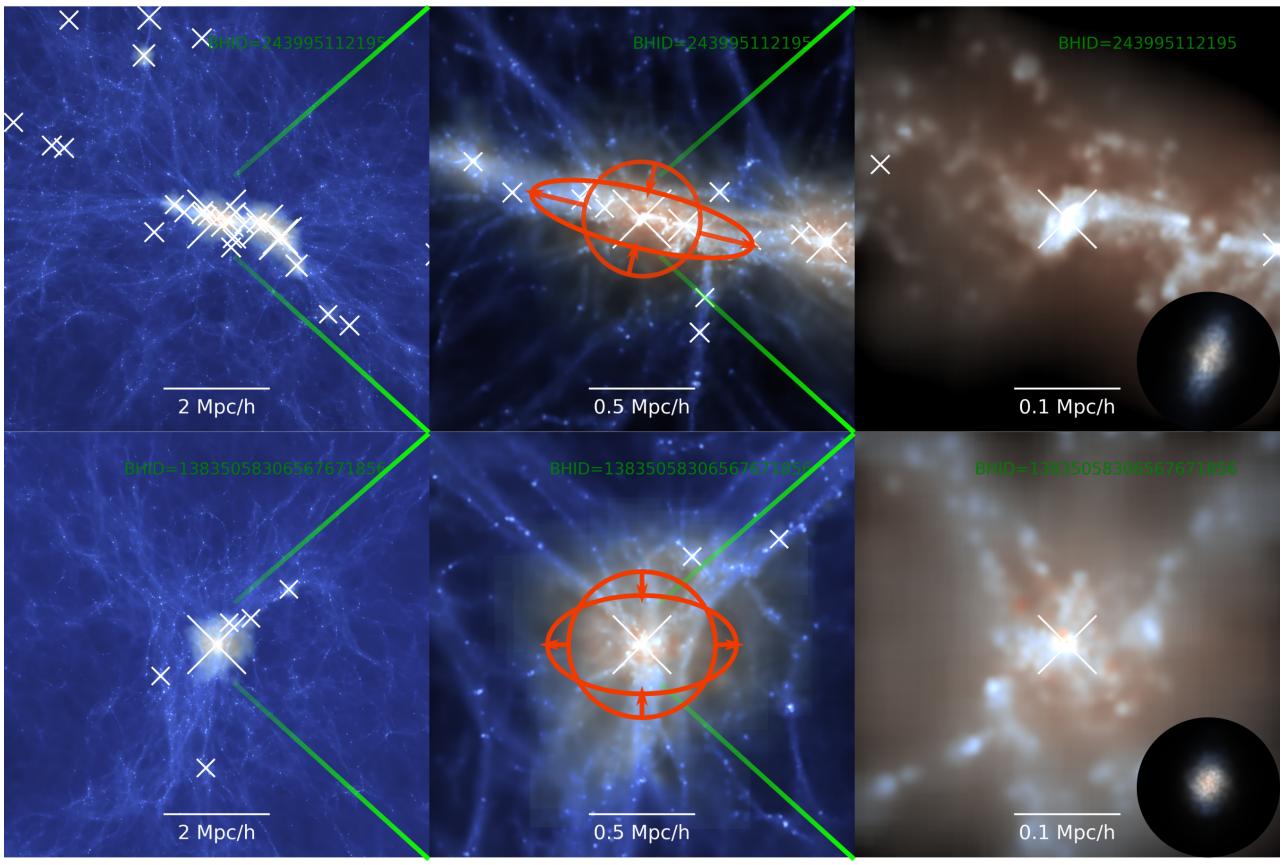

Figure 3. Same as Figure 2. The most massive disk galaxy environment (top row) compared to the most massive black hole and host galaxy (bottom row). The orange ellipses and arrow illustrate the tidal field $t1$ and $t3$ in the two cases. Tidal fiels stretches material along $t1$ and compresses material along $t3$. Strong fields, large $t1$ is found in the large scale filament in the environment of the disk galaxy and small $t1$ and associated thin, 'cold' filaments are characteristic of the enviroments of the most massive BHs.

Property	BH1	BH2	BH3	BH4
$M_{BH}(\times 10^8\,\mathrm{M}_\odot)$	4.1	1.5	0.9	0.8
$M_{200}(\times 10^{10}\,\mathrm{M}_\odot)$	42	33	44	92
$M_{\rm star}(\times 10^{10}\,\mathrm{M}_\odot)$	3.7	2.5	4.1	5.7
$M_{\rm gas}(\times 10^{10}\,\mathrm{M}_\odot)$	4.0	3.9	4.9	13
$f_{gas}[M_{\rm gas}/(M_{\rm gas}+M_{\rm star})]$	0.5	0.6	0.6	0.7
D/T	0.2	0.1	0.5	0.5
$t1$ (tidal field)	0.29	0.23	0.32	0.08

Table 1. Basic properties of the four most massive black holes and their hosts at $z = 8$. Images of the environments and host galaxies of these objects are shown in Fig. 2.

plain the extremely massive rare objects that are seen. This rapid growth is consistent with the black hole leading galactic growth through early assembly.

Figure 5 tracks directly the evolution of the black hole mass and accretion rate for the four most massive black holes (solid lines) and those of the most massive, disky stellar systems. As expected, the black holes that build up the largest masses accrete close to their critical Eddington accretion rate virtually since the time they were seeded. This can be seen as the curves are close to flat for most of the cosmic time. Note however that the black holes are not exclusively following the Eddington rate but show some variability, with peaks and troughs while remaining close to that value. These are a result of the complex interplay of AGN feedback in the gas. While feedback is unable to quench and completely heat and remove the accreting gas the inflows are disturbed and accretion rate has significant variations particularly toward lower redshifts ($z \sim 8$). In the left panel of Figure 5 we can see that at this epoch black hole mass is still growing steeply, with no sign that it has saturated at its final value. This is consistent with observations of SDSS quasars which have implied masses close to $10^9\,\mathrm{M}_\odot$ at $z \sim 6$ (Di Matteo et al. 2012, see also). From the right panel of Figure 5 we can see that the BH accretion rates in disk-dominated objects are about an order of magnitude lower than in the most massive black hole sample.

In Figure 6 we turn to the evolution of the associated D/T ratio and SFR of the host galaxies of the massive black holes and massive disks discussed in Figure 5.

We have seen (Fig. 1 and Fig. 2 that the most massive black holes are typically associated with spheroid-dominated hosts at $z = 8$. Figure 6 shows that indeed the D/T ratios are typically small for the hosts of massive black holes and in particular that D/T generally stays small with redshift (at least over the redshift range we can access with BlueTides). It is also interesting to note that while the typical SFRs are pretty high at the highest redshifts for the massive black holes in the spheroid-dominated hosts, they do not increase

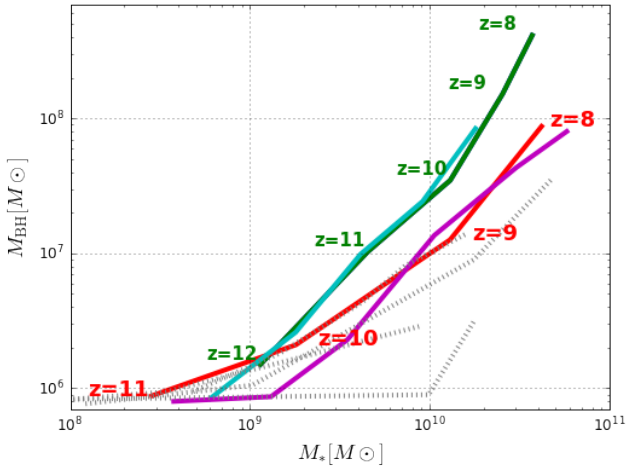

Figure 4. The Coevolution of blackhole mass and stellar mass in the four most massive black holes (solid lines) compared to four of the most massive disks (dashed lines). Black hole growth is faster in the the spheroid-dominated objects compared to the growth in disk-dominated galaxies.

by much at low redshifts. For the disk-dominated massive hosts on the other hand, the star formation rates increase rapidly, reaching up to several $1000\,{\rm M}_\odot$/yr, up to factors 50 higher than in the massive black hole hosts. It appears therefore that the presence and fast growth of a massive black hole in these early compact spheroids is able to quench (through its associated feedback) the SFR in the massive black hole hosts. This somewhat evident also Fig. 2 where the stellar population in the central region of the spheroid is rather old (shown by the the ref colors). We note however even at these high-z gas rich environments the SFR are still a few hundred ${\rm M}_\odot/yr$.

3.3 The origin of the fastest black hole growth: tidal field strength

Our results so far suggest that the growth of the most massive, early black holes in BlueTides is linked to mechanisms operating on and related to the formation of their hosts and not to the occurrence of major mergers. It also appears that the galaxy morphology at these epochs is related to black hole growth. Whether a galaxy is disk-like or spheroidal is imprinted early on and not the result of a sudden accretion/merger driven transformation. These considerations and the visual differences in the large-scale distribution of surrounding matter (illustrated by Figure 3) in regions surrounding host galaxies with rapid black hole growth versus regions inducive of early disk formation suggest that net angular momentum and the impact of tidal field strength in these regions may play a role. In particular, we see that the large-scale distribution of the gas around the massive black holes is typically composed of thin, distinct filaments which do not interact and which lead to fast 'cold' gas accretion to prevail forming a spheroid host. The formation of spheroids in these environments has been seen in earlier work (Sales et al. 2012). In that work it was also suggested that galaxy morphology was related to spin alignment of accreting matter: the coherent alignment of the net spin and hence similar angular momentum leads to disk dominated systems whereas the direct filamentary accretion of gold gas is accompanied by spin misalignments and favors the formation of spheroids.

Along these lines, here we study the relation between the tidal field and spheroids with early massive black holes and the suppressed early growth of black holes in regions of disk formation. As an illustration, we show that indeed where tidal fields are large ($t1 = 0.6$), a large scale filament forms (see Figure 3). This induces significant tangential motion in the accreting gas, leading to high angular momentum and the formation of a massive early disk. Conversely the tidal field strength is low $t1 = 0.2$ in regions with thin converging filaments which bring in cold material fast and lead to the formation of the most massive black hole in a spheroidal dominated host. Tidal torque theory has been shown by Gonzalez et al. (2016) to explain the initial spin of galaxies in hydrodynamic simulations at high redshifts, and Prieto et al. (2015) have found that halos with fewer filaments tend to have larger spin. This is in agreement with the examples we have presented here, where the disc galaxies tend to lie in regions with two main filaments, and the low angular momentum galaxies that host black holes lie at the centers of a more symmetric arrangement of multiple filaments.

We now move on from these illustrative examples to investigate whether these results also apply statistically to the galaxy morphology and black holes accretion rates of the entire sample of massive galaxies in BLueTides. We measure the tidal field strength for the 22156 galaxies with stellar masses $> 10^8\,{\rm M}_\odot$) that host a black hole at $z = 8$. In Figure 7 we plot the mean D/T ratio and Eddington accretion rate as a function of the tidal field strength $t1$ (measured at a scale of 1 Mpc)

We can see in the left panel of Figure 7 that the mean D/T ratio for the galaxies in BlueTidesdoes show a strong dependence on tidal field strength. As seen in the examples above, the large tidal field environments induce coherent acquisition of angular momentum and hence disk formation. Conversely, in the right panel of Figure 7 we find that on average the largest black hole accretion rates are induced in regions with the smallest tidal fields. This is consistent with the fastest black hole growth at these early times being associated to those region in which gas is accreted cold and fast through direct filamentary accretion. The most massive black holes thus may form even in the absence of mergers.

We quantify these relationships in two fashions. First, we compute the Spearman rank correlation coefficient r_s between t and D/T ratio and between t and Eddington accretion rate. We find $r_s \sim 0.1$ and $r_s \sim -0.05$, respectively with very high significance (see the results in Table 2) This indicates that although there is scatter about the relation, there is an extremely significant correlation between t and D/T and an anti-correlation between t and accretion rate. We have also fit a simple linear relation between the values of D/T averaged in bins of t and a linear fit to the Eddington accretion values in bins of t also yields an acceptable. The parameters for these fits are also given in Table 2.

These quantitative results confirm our earlier suggestion that regions of significant tidal field strength hosting early massive galaxies preferentially lead to the formation of disks, while the lowest tidal fields lead on average to the

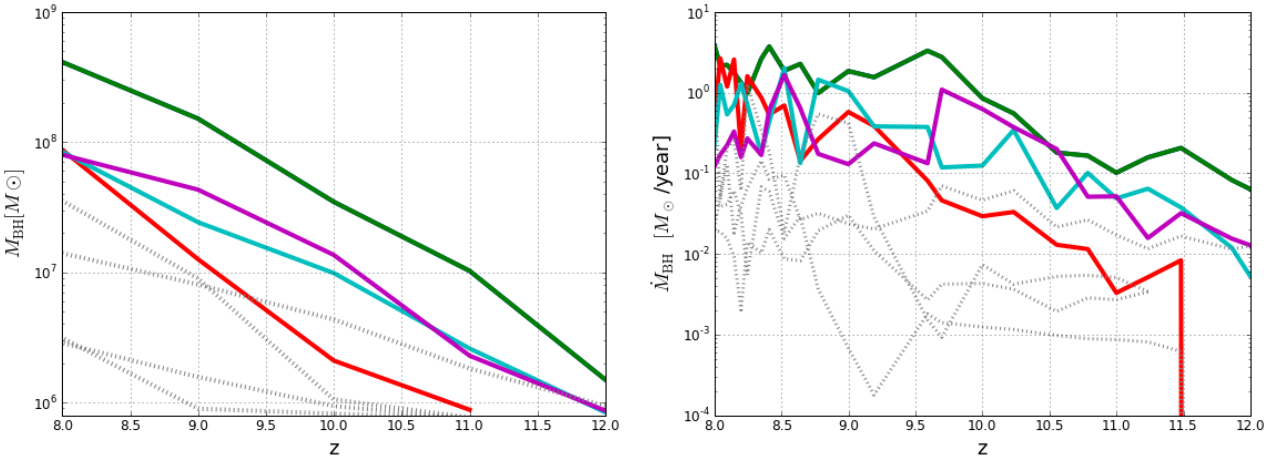

Figure 5. The evolution of blackhole and accretion rate. Solid lines: blackhole mass and corresponding accretion rate for the most massive blackholes at $z = 8$. Dashed lines: a sample of the black holes in the most disk-dominated galaxies at $z = 8$.

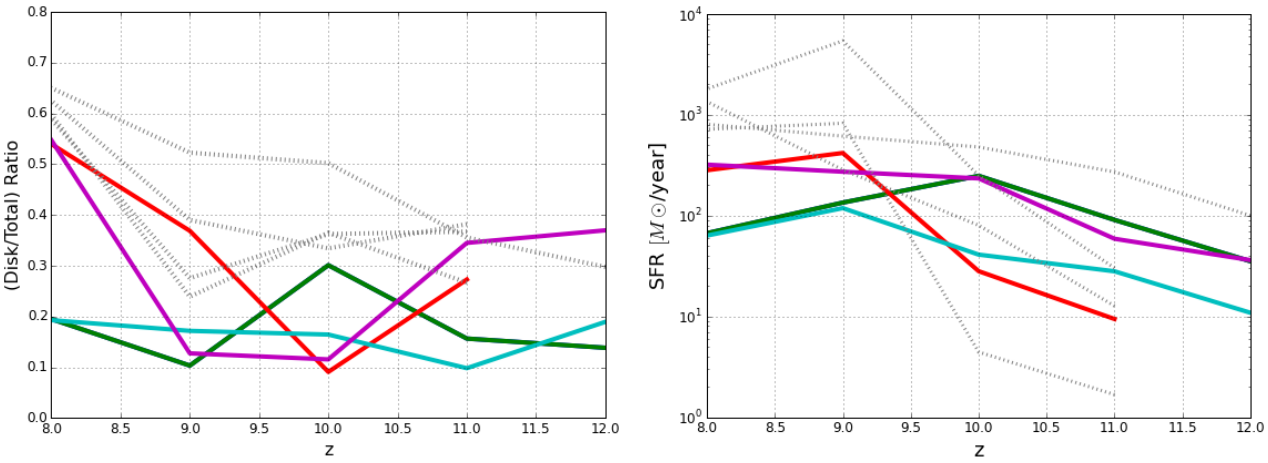

Figure 6. The D/T ratio for the host galaxies for black holes in Fig. 5. The solid lines and dashed lines correspond to those in Fig. 5.

more significant cold accretion and black hole growth, and which is associated with the formation of spheroid dominated systems.

4 CONCLUSIONS

We use the hydrodynamical cosmological simulation BLUETIDESto study the origin of the most massive black holes at early times. Here we have focussed our analysis on the massive galaxies and black holes at $z \geqslant 8$ (for earlier discussion of $z = 6$ SDSS quasars, see e.g. Di Matteo et al. 2012; Feng et al. 2014). In Feng et al. (2015) we discussed how the most massive galaxies at these epochs are likely disk dominated. Here we have shown that while the most massive disks can still host massive black holes the most extreme early black hole growth (reaching a $M_{\rm BH}$ a few $10^8\,{\rm M}_\odot$ at $z = 8$) occurs in spheroid-dominated extremely compact galaxies. The sites of extremely rapid black hole growth hosted by spheroid-dominated galaxies are the result of large-scale filamentary accretion of cold gas from which the halo and eventually black holes can accrete new material radially (at low angular momentum). The large scale, thin filamentary structures surrounding these halo is a direct result of the relatively low tidal field strength due to the surrounding large-scale density field. In contrast, for halos located in strong tidal fields, the surrounding filamentary structure is larger than the halo allowing material to be accreted from different directions producing more gradual accretion (deceleration along $t1$) parallel to the large scale filament - and acceleration (along $t3$) - perpendicular to the filaments, allowing material to accrete angular momentum more coherently.

We find that star formation in the spheroidal hosts of massive BHs prompts very rapid transformation of gas into stars and with BH feedback heating and somewhat quenching the inner regions which result in an older stellar populations. Disk dominated hosts tend to have even higher star formation rates (less quenched by AGN feedback) and which arise after a gradual ramp up in time as gas accretion is somewhat delayed compared to the spheroids. We plan to explore the observational signatures of these populations

Property	a	b	r_s	Δ
Galaxy D/T	9.75×10^{-2}	3.6	8.7×10^{-2}	1.4×10^{-38}
BH Eddington	0.22	6.12×10^{-2}	-4.94×10^{-2}	1.78×10^{-13}

Table 2. Parameters a, and b for a linear fit in the correlations between D/T ratio and BH Eddington accretion rate versus tidal field strength $t1$ shown in Fig. 7. The spearman rank correlation coefficient r_s and Δ the two sided significance of its deviation from zero. Here small values indicate more significant correlations.

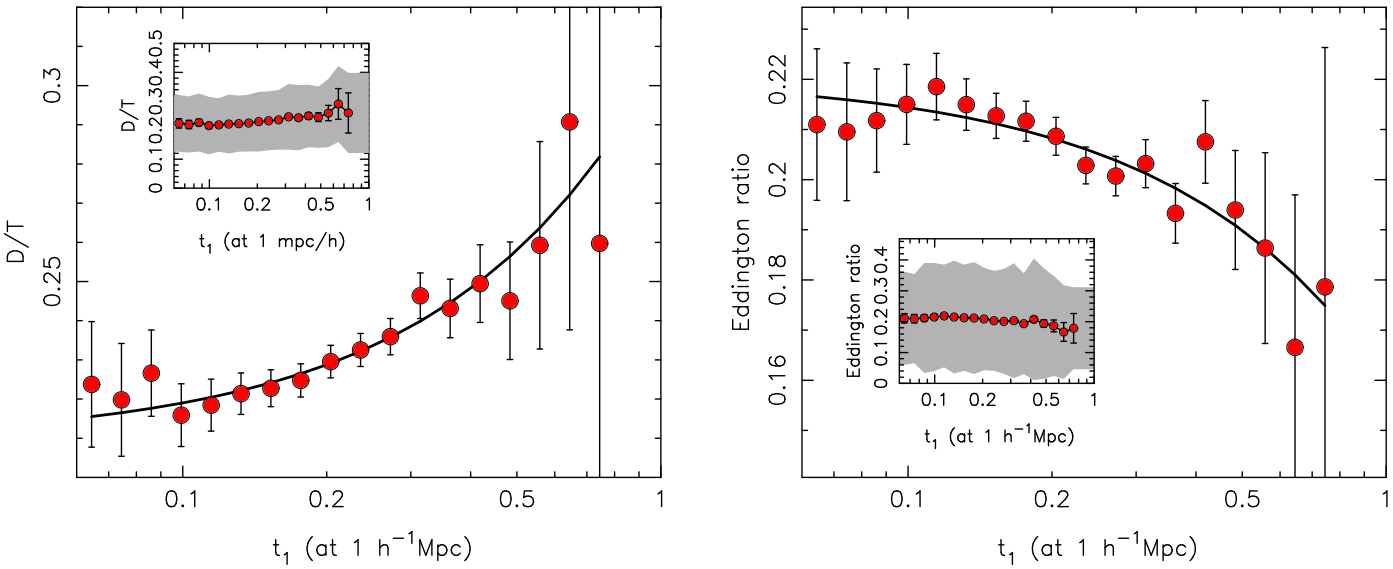

Figure 7. Left: The disk-to-total ratio for BlueTidesBH host galaxies versus t_1, the tidal field strength. Right: the Eddington accretion rate of BHs versus t_1. The inset panels in each case show the same data, but with an increased y-axis range. The points with error bars show the mean values of D/T and Eddington ratio in bins of t_1. The error bar is the error on the mean, and the shaded regions indicate the range which encloses 68% of the galaxies in each bin. The smooth curves are linear fits of D/T and Eddington ratio to t_1, with the fit parameters given in Table 2

of stars in the most massive disks versus the most massive black hole hosts in future work.

Our results suggest a new scenario for the origin of the most massive early black holes which does not rely on major gas rich mergers. This scenario offers clues to the origin of the most massive, rare high-z black holes. These extreme black holes can be grown at the highest rates in high density regions in the early Universe but not necessarily the most extreme ones: what is important is that they grow most rapidly in regions with relatively low tidal fields due to their environments. The fact that the brightest quasars at these early times host the most massive black holes, but do not necessarily have to live in the densest regions of the universe, imply that they are unlikely to be the precursors of the massive black holes in cluster of galaxies today. More likely their descendants will not be in privileged sites but in rather isolated galaxies (e.g. Thomas et al. 2016)

Our work and the finding that black hole growth is linked to tidal field theory offers some explanation as to the origin of the most massive BHs in most compact galaxies. It is interesting that Barber et al. (2016) using the EAGLE simulation at $z = 0$ also found a strong link between compactness of the host and the most (positive) outliers in the $M_{\rm BH} - M_*$ relation. These authors also find that the most extreme outliers grow rapidly in $M_{\rm BH}$ at early times to to lie well above the present day $M_{\rm BH} - M_*$ relation and are consistent with undisturbed morphologies implied by late time observations. In the context of our findings it is likely that indeed the most extreme massive black hole outliers are linked to regions with lower tidal fields in the initial conditions. While it is currently unfeasible (with any current HPC) to run BlueTidesto $z = 0$, we also plan to carry out a Dark-Matter Only BlueTideswhich will allow us to study the descendants of the the earliest supermassive BHs.

The fastest black hole growth is then a direct consequence of the initial conditions of the density field. Although the limited time evolution and somewhat limited numerical resolution of the large volumes of BlueTidesprecludes more detailed studies and investigations we plan to use these clues to re-simulate some of these systems at higher resolution (Feng et al. 2014, as we did with MB simulation, see e.g.) with the goal of studying in more detail the dependence and constrain seed black hole scenarios. We note that (Danovich et al. 2015, and references therein) have studied in detail the angular-momentum buildup in $high - z$ massive galaxies using high-resolution zoom cosmological simulations and have explicitly studied the link with early disc formation and tidal field theory. In our work we illustrate that black hole formation and angular momentum buildup can be understood within the same context.

5 ACKNOWLEDGEMENTS

We thank Y. Dubois and M. Volonteri for early discussion on the importance of angular momentum build-up for early, massive BH formation. We acknowledge funding from NSF ACI-1036211, NSF ACI-1614853, NSF AST-1517593, NSF AST-1009781, and the BlueWaters PAID program. The BlueTides simulation was run on facilities on BlueWaters at the National Center for Supercomputing Applications. SMW acknowledges support from the UK Science and Technology Facilities Council.

References

Abel T., Bryan G. L., Norman M. L., 2000, ApJ, 540, 39
Barber C., Schaye J., Bower R. G., Crain R. A., Schaller M., Theuns T., 2016, MNRAS, 460, 1147
Battaglia N., Trac H., Cen R., Loeb A., 2013, ApJ, 776, 81
Begelman M. C., Volonteri M., Rees M. J., 2006, MNRAS, 370, 289
Bouwens R. J. et al., 2015, ApJ, 803, 34
Bromm V., Coppi P. S., Larson R. B., 1999, ApJ, 527, L5
Dalal N., White M., Bond J. R., Shirokov A., 2008, ApJ, 687, 12
Danovich M., Dekel A., Hahn O., Ceverino D., Primack J., 2015, MNRAS, 449, 2087
Di Matteo T., Khandai N., DeGraf C., Feng Y., Croft R. A. C., Lopez J., Springel V., 2012, ApJ, 745, L29
Di Matteo T., Springel V., Hernquist L., 2005, Nature, 433, 604
Fan X. et al., 2006, AJ, 132, 117
Faucher-Giguère C.-A., Lidz A., Zaldarriaga M., Hernquist L., 2009, ApJ, 703, 1416
Feng Y., Di Matteo T., Croft R., Khandai N., 2014, MNRAS, 440, 1865
Feng Y., Di Matteo T., Croft R., Tenneti A., Bird S., Battaglia N., Wilkins S., 2015, ApJ, 808, L17
Feng Y., Di-Matteo T., Croft R. A., Bird S., Battaglia N., Wilkins S., 2016, MNRAS, 455, 2778
Fioc M., Rocca-Volmerange B., 1997, A&A, 326, 950
Gao L., Able T., Frenk A., A. J., V. S., N. Y., 2006, MNRAS
Gonzalez R. E., Prieto J., Padilla N., Jimenez R., 2016, ArXiv e-prints
Hinshaw G. et al., 2013, ApJS, 208, 19
Hockney R. W., Eastwood J. W., 1981, Computer Simulation Using Particles
Jiang L. et al., 2009, AJ, 138, 305
Katz N., Weinberg D. H., Hernquist L., 1996, ApJS, 105, 19
Koushiappas S. M., Bullock J. S., Dekel A., 2004, MNRAS, 354, 292
Krumholz M. R., Gnedin N. Y., 2011, ApJ, 729, 36
Mortlock D. J. et al., 2011, ArXiv e-prints
Nakamura F., Umemura M., 2001, ApJ, 548, 19
Nelson D. et al., 2015, Astronomy and Computing, 13, 12
Prieto J., Jimenez R., Haiman Z., González R. E., 2015, MNRAS, 452, 784
Sales L. V., Navarro J. F., Theuns T., Schaye J., White S. D. M., Frenk C. S., Crain R. A., Dalla Vecchia C., 2012, MNRAS, 423, 1544
Schaye J. et al., 2015, MNRAS, 446, 521
Song M. et al., 2015, ArXiv e-prints
Springel V., Hernquist L., 2003, MNRAS, 339, 289
Thomas J., Ma C.-P., McConnell N. J., Greene J. E., Blakeslee J. P., Janish R., 2016, Nature, 532, 340
Vogelsberger M., Genel S., Sijacki D., Torrey P., Springel V., Hernquist L., 2013, MNRAS, 436, 3031
Vogelsberger M. et al., 2014, MNRAS, 444, 1518
Wang H., Mo H. J., Jing Y. P., Yang X., Wang Y., 2011, MNRAS, 413, 1973
Waters D., Di Matteo T., Feng Y., Wilkins S. M., Croft R. A. C., 2016a, ArXiv e-prints
Waters D., Wilkins S., Di Matteo T., Feng Y., Croft R., Nagai D., 2016b, ArXiv e-prints
Wilkins S. M., Feng Y., Di-Matteo T., Croft R., D. W., 2016a, MNRAS
Wilkins S. M., Feng Y., Di-Matteo T., Croft R., Stanway E. R., Bouwens R. J., Thomas P., 2016b, MNRAS, 458, L6
Wilkins S. M., Feng Y., Di-Matteo T., Croft R., Stanway E. R., Bunker A., Waters D., Lovell C., 2016c, ArXiv e-prints
Yoshida N., Sokasian A., Hernquist L., Springel V., 2003, ApJ, 598, 73